



Multiple Engine Faults Detection Based on Variational Mode Decomposition and Echo State Network

Xin Li and Fengrong Bi Tianjin University

Xiaoqiang Ma Tianjin Internal Combustion Engine Research Institute

Pengfei Shen and Jiangang Cheng Tianjin University

Citation: Li, X., Bi, F., Ma, X., Shen, P. et al., "Multiple Engine Faults Detection Based on Variational Mode Decomposition and Echo State Network," SAE Technical Paper 2020-01-0418, 2020, doi:10.4271/2020-01-0418.

Abstract

As a major power source, diesel engines are being widely used in a variety of fields. However, because of complex structure, some faults which cannot be detected by direct signals would occur on engines and even lead to accidents. Among all kinds of indirect signals, vibration signal is the most common choice for faults detection without disassemble because of its convenience and stability. This paper proposed a novel approach for detecting multiple engine faults based on block vibration signals using variational mode decomposition (VMD) and echo state network (ESN). Since the quadratic penalty has a great influence on adaptable VMD that may make expected component signals cannot be extracted exactly, this paper proposed a dynamic quadratic penalty value, which will change with decomposing

level. This paper selected a best dynamic quadratic penalty value by analyzing a large amount of data and results showed that this approach can decompose signals more exactly. Based on that, 8 characteristic parameters were extracted to describe faults features comprehensively, while high-dimensional data raised computational difficulty for classifier. To improve the recognition rate of ESN for high-dimensional data, this paper proposed an approach that using dimensionality reduction method, in which the kernel local Fisher discriminant analysis (KLFDA) based on Gauss kernel function was proved to be the best choice, to reduce the dimension of original data firstly. Then the ESN was used to recognize faults by analyzing the low-dimensional data. Results showed that this approach obtained ideal recognition rate and had ability to detect multiple engine faults exactly.

Introduction

As a main power source, diesel engines are being widely used in industry, agriculture and so on because of their high output power, fuel economy and safety. Especially for ships, offshore oil platforms and other special industries, diesel engine is the only conventional power source [1]. Under the increasingly outstanding energy and environment issues, a series of technologies, such as high-pressure common-rail fuel system and exhaust gas recirculation (EGR), have been used in diesel engine to meet the requirements of law. On one hand, the technologies can improve performance, on the other hand, the increasingly complexity of diesel engine causes higher probability of failure [2]. The performance of engine has great influence on whole system, which forces researchers to search accurate and efficient fault detection methods in order to protect the safety of life and property [3].

At the present stage, several fault detection methods such as monitoring performance parameters [4], analyzing oil [5], detecting noise [6] and detecting vibration [7] are being widely used. Among these, performance parameters only contain direct signals, which cannot recognize most of the mechanical faults. Analyzing the physico-chemical characters of particulates in oil is carried after stopping, which cannot realize real time

diagnosis. Detecting noise is easily influenced by external factors and has low accuracy. Detecting vibration signals is being a major field of research because of stability and convenience.

Owing to complex engine structure, there is so much noise in vibration signals that signal processing methods are employed to detect faults feature. Faults detection includes decomposing feature components, extracting characteristic parameters and faults recognition. When decomposing feature components, time-frequency analysis algorithm is the most frequently used method, which is represented by short time Fourier transform (STFT), wavelet transform and empirical mode decomposition (EMD). Sharma et al analyzed vibration signals of cylinder head by STFT and designed a system to detect misfire [8]. Alireza et al combined discrete wavelet transform and energy spectrum to analyze intake manifold vibration signals and obtained more accurate results in fuel injection fault detection [9]. Ma et al applied EMD to decompose engine vibration signals and recognized knock in different intensities [10]. However, STFT cannot reach high resolution both in time and frequency domains. Wavelet transform just decomposes signals mechanically in frequency domain. Because of the shortcomings of recursive model, mode mixing and low robustness for close frequencies are still

the major problems in EMD. Although ensemble empirical mode decomposition (EEMD) can solve these problems to a certain extent, the following residual white noise and low efficiency limit its application [11, 12]. In 2014, Dragomiretskiy et al proposed variational mode decomposition (VMD) based on variational model instead of recursive model [13]. VMD has higher accuracy and efficiency and shows great potential in faults detection, for example, Ren et al used VMD to detect diesel engine crankshaft bearing fault [14]. However, the result of VMD is influenced by several control parameters, especially decomposing level and quadratic penalty have to be selected manually, which reduces the accuracy and efficiency of VMD.

Fuzzy c-means (FCM), support vector machine (SVM) and artificial neural network (ANN) are common classifiers to recognize faults after decomposition and characteristic parameters extraction. FCM was used by Bi et al to classify engine valve and fuel injection failures [15]. Wang et al used SVM to recognize the data processed by mixed kernel function and sparse decomposition, and the results showed this method could detect early weak faults of high-speed aero-engine's bearings [16]. Zheng et al proposed a state observer method for gasoline engine using Luenberger and sliding mode technique, and then back-propagation neural network (BPNN) was employed to detect misfire fault based on that [17]. However, FCM is an unsupervised classifier, which cannot make use of expert knowledge. Multi-class SVM is built based on several 2-class classifiers and the complex structure brings low calculation efficiency and accuracy. Classical ANN is not only easy to fall into local optimum but also has slow convergence speed because of the nature of gradient descent method in training. In 2004, Jeager et al proposed echo state network (ESN) [18]. The basic principle of ESN is taking a random generated reservoir, instead of hidden layer neurons, as basic processing unit to transform calculation into a linear regression problem, which can overcome the local optimum and low efficiency significantly. However, ESN is often used in prediction and there is much research need to do in pattern recognition [19].

This paper is organized as follows. This section introduces the research background and significance. The second section introduces the algorithms briefly. The experiment is described in the third section. VMD is optimized in the fourth section. ENS is optimized in the fifth section. The last section summarizes this paper and discusses the research directions in the future.

Algorithm Theories

VMD and ESN are the two main algorithms for this work and they are introduced in this section.

VMD Theory

The goal of VMD is to decompose input signal into several discrete modal components with specific sparsity. The modal component is supposed to compact around a center frequency ω_k [13].

Suppose f is input signal, u_k is modal component that is intrinsic mode function (IMF). The unilateral spectrum of u_k is calculated by Hilbert transform firstly.

$$H = \left[\delta(t) + \frac{j}{\pi t} \right] u_k(t) \quad (1)$$

where δ represents Fermi-Dirac distribution and $j^2 = -1$

The u_k can transform into baseband by mixing a center frequency, which in VMD is estimated as $e^{-j\omega_k t}$.

$$B = \left[\delta(t) + \frac{j}{\pi t} \right] u_k(t) * e^{-j\omega_k t} \quad (2)$$

where $*$ represents convolution, e refers to the base of natural logarithms.

The bandwidth of u_k could be estimated by Gaussian smoothness. Considering the relationship between u_k and f , a constrained variational model can be built as:

$$\left\{ \begin{array}{l} \min_{\{u_k\}, \{\omega_k\}} \left\{ \sum_k \left\| \partial_t \left[\delta(t) + \frac{j}{\pi t} \right] u_k(t) * e^{-j\omega_k t} \right\|_2^2 \right\} \\ s.t. \sum_k u_k = f \end{array} \right. \quad (3)$$

where $\{u_k\} := \{u_1, u_2, \dots, u_k\}$ and $\{\omega_k\} := \{\omega_1, \omega_2, \dots, \omega_k\}$ represent

all IMFs and their center frequencies, respectively. $\sum_k := \sum_{k=1}^k$

is the summation of all the IMFs.

Quadratic penalty α and Lagrangian multipliers λ are introduced into Equation (3) to transform the constrained variational model into unconstrained.

$$L(\{u_k\}, \{\omega_k\}, \lambda) := \alpha \sum_k \left\| \partial_t \left[\left(\delta(t) + \frac{j}{\pi t} \right) * u_k(t) \right] e^{-j\omega_k t} \right\|_2^2 + \dots \quad (4)$$

$$+ \left\| f(t) - \sum_k u_k(t) \right\|_2^2 + \lambda(t), f(t) - \sum_k u_k(t)$$

The quadratic penalty is used to control reconstruction fidelity, especially for high noise level. The weight of quadratic penalty should increase with noise reducing and vice versa. Lagrangian multiplier is a classic method to enforce constraints strictly.

The Equation (4) can be solved as:

$$\hat{u}_k^{n+1}(\omega) = \frac{\hat{f}(\omega) - \sum_{i \neq k} \hat{u}_i(\omega) + \frac{\hat{\lambda}(\omega)}{2}}{1 + 2\alpha(\omega - \omega_k)^2} \quad (5)$$

$$\omega_k^{n+1} = \frac{\int_0^\infty \omega |\hat{u}_k(\omega)|^2 d\omega}{\int_0^\infty |\hat{u}_k(\omega)|^2 d\omega} \quad (6)$$

$$\hat{\lambda}^{n+1}(\omega) = \hat{\lambda}^n(\omega) + \tau \left(\hat{f}(\omega) - \sum_k u_k^{n+1} \right) \quad (7)$$

where τ refers to update parameter. When the noise in signal is much and the reconstruction accuracy is not severe demand, the τ can be set as 0 to use the quadratic penalty only.

The detailed calculation steps are as follows:

1. Initialize $\{\hat{u}_k^1\}$, $\{\omega_k^1\}$ and $\hat{\lambda}^1$.
2. Solve u_k, ω_k and λ by alternate direction method of multipliers (ADMM) based on Equation (5), (6) and (7), respectively.
3. Repeat above process until meeting stopping condition. In VMD, the stopping condition is set as:

$$\sum_k \|\hat{u}_k^{n+1} - \hat{u}_k^n\|_2^2 / \|\hat{u}_k^n\|_2^2 < \varepsilon \quad (8)$$

where $\varepsilon = 10^{-7}$ is the default value.

ENS Theory

ENS is a new type of recurrent neural network (RNN). The main characteristic of ESN is replacing hidden layer neurons by a random generated reservoir. It also has high efficiency because only output weight matrix needs training, which is a simple linear regression problem [18]. The basic principle of ENS is described as Fig. 1.

The state equation of reservoir is:

$$x(t+1) = f_r(W_{in}u(t+1)) + Wx(t) + W_{back}y(t) \quad (9)$$

where $x(t)$ is the state vector of reservoir, $u(t)$ and $y(t)$ are input vector and output vector, respectively, the t is state parameter. $f_r(\cdot)$ refers to the activation function of reservoir. W_{in} , W_{back} and W are the weight matrixes of input, feedback and reservoir internal connection, respectively.

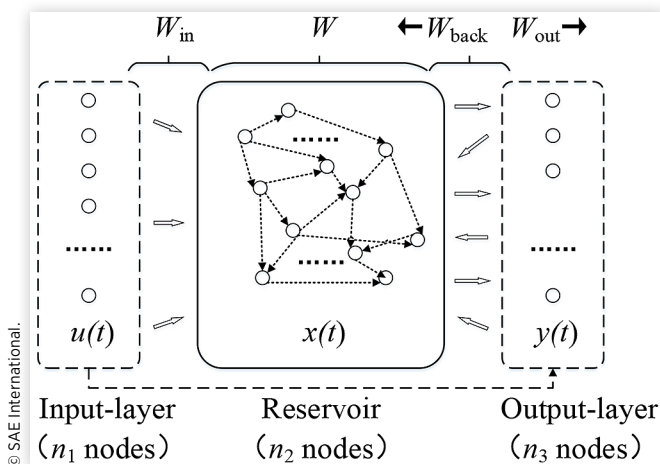
The output of ESN is:

$$y(t+1) = f_{out}(W_{out}u(t+1)), x(t+1), y(t) \quad (10)$$

where W_{out} represents output weight matrix, $f_{out}(\cdot)$ represents output activation function.

The reservoir is dynamic space, which can output required result if it is complex enough. The output weight matrix is trained after initialization and the output nodes are adjusted based on minimum mean square error (MMSE).

FIGURE 1 Basic principle of ENS.



Engine Bench Test

The engine fault experiment was performed on a turbocharged 6-cylinder in-line diesel engine. Engine detailed parameters are listed in Table 1.

The engine was connected rigidly to test bench, which was supported by 4 air springs and the natural frequency of supporting system was below 2 Hz. The acceleration sensors were installed on cylinder head to collect vibration signals. The photoelectric rotating-speed sensor was placed near the connecting shaft of dynamometer to locate the top dead center. The testing equipments are shown in Table 2.

The testing bench is shown as Fig. 2. To cover the fault feature frequency (mainly distributes within 10 kHz), the sampling frequency was set as 25.6 kHz based on the comprehensive consideration of Nyquist sampling theorem and the filtering characteristics of testing system.

The engine load conditions were set as 100%, 75%, 50% and 25%, the speed conditions were set as 2300 r/min, 2100 r/min, 1600 r/min, 1300 r/min and 700 r/min. As idle speed, the working condition of 700 r/min was also tested at 0% load.

TABLE 1 Main parameters of tested engine.

Items	Parameters
Displacement	7.14L
Firing sequences	1-5-3-6-2-4
Rated Power	220kW@2300r/min
Maximum Torque	1250Nm@1200-1600r/min

© SAE International.

TABLE 2 Main parameters of testing equipment.

Instrument	Model	Manufacturer
Data collector	LMS Scada III	Siemens
Acceleration sensor	621B40	IMI SENSORS
Photoelectric rotating-speed sensor	SPSR-115	MONARCH
Laptop computer	Thinkpad T530	Lenovo

© SAE International.

FIGURE 2a Testing bench.

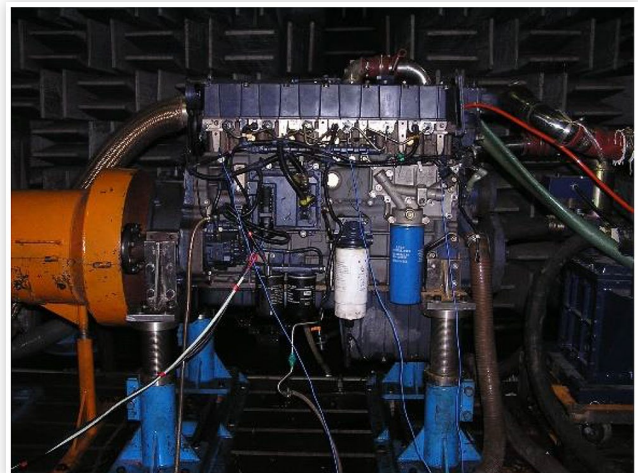


FIGURE 2b Vibration sensors.

© SAE International.

FIGURE 2c Testing equipment.

© SAE International.

As common faults, injection system failure and valve system failure were researched in experiment. For injection system failure, the injection quantity was reduced to 75% of normal condition. For valve system failure, the intake and exhaust valve clearances were adjusted to 0.25 mm and 0.45 mm respectively to simulate small valve clearance, and adjusted to 0.40 mm and 0.60 mm respectively to simulate big valve clearance. In normal condition, the intake and exhaust valve clearances are 0.30 mm and 0.50 mm respectively. These failures were adjusted cylinder by cylinder.

Adaptable VMD with Dynamic Quadratic Penalty

Adaptable VMD Algorithm

As mentioned above, decomposing level K and dynamic quadratic penalty α are the most important parameters in VMD, while they are selected subjectively. For the

decomposing level K , authors' team proposed an adaptable VMD and it is shown as follows [20]:

1. Compute the power spectral density (PSD) of input signal f , and take the peak frequency as $\omega_{\max 1}$.
2. Set the decomposing level K as 1, and take the $\omega_{\max 1}$ as iterative initial center frequency to decompose the input signal f . Take the only one component as IMF1.
3. Let $f_2 = f - \text{IMF1}$ and repeat steps ①-② to get IMF2. The rest IMFs also can be obtained by analogy.
4. Let the energy of the k th component IMF $_k$ be E_k , the energy of residual signal ($f_k - \text{IMF}_k$) be E_{re} , the energy of the k th input signal f_k be E_f . Energy difference is: $E_{err} = |E_k + E_{re} - E_f|$. Based on energy difference tracking method, the orthogonality of result increases with the E_{err} reducing, which is able to be the stopping condition of adaptable VMD. Let the energy of original input signal f be E_{tot} and the

stopping condition is usually set as $r = \frac{E_{err}}{E_{tot}}$, where

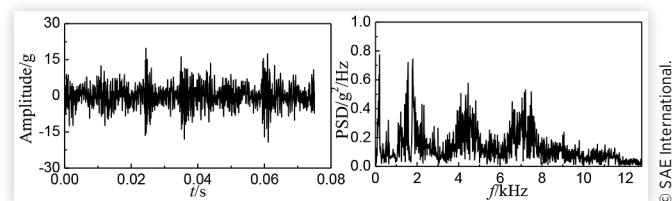
$r \in [0.5\%, 1.5\%]$ is appropriate.

The above method can decompose signals without predefined decomposing level. To verify it, a real vibration signal at 1600r/min with 100% load was decomposed by adaptable VMD and EMD, respectively. The signal was measured from Y direction (the horizontal direction perpendicular to crankshaft) near the first cylinder. The time and frequency domains of input signal are shown in Fig. 3, all the 6 IMFs automatically derived from adaptable VMD are shown in Fig. 4 and 6 of 10 IMFs in EMD result are shown in Fig. 5 (the last 4 components are obviously illusive components). By the way, the stopping condition of adaptable VMD was set as 1.0%, and the same value was adopted in following sections. The quadratic penalty α was set as 2000.

As shown in Fig. 4, almost ideal narrow bandwidth signals are extracted by adaptable VMD and the components with different frequencies are distinguished clearly. As to the result of EMD in Fig. 5, the frequency components of IMF1 and IMF2 are complex, which has an adverse effect on faults detection. Besides, the result of VMD is simpler and more efficient, which can be concluded that the adaptable VMD is more appropriate for engine faults detection.

Dynamic Quadratic Penalty

Quadratic penalty is another important parameter in VMD. As shown in Fig. 4, frequency overlaps can be found between

FIGURE 3 Time and frequency domains of measured signal.

© SAE International.

FIGURE 4 Time and frequency domain results of adaptable VMD.

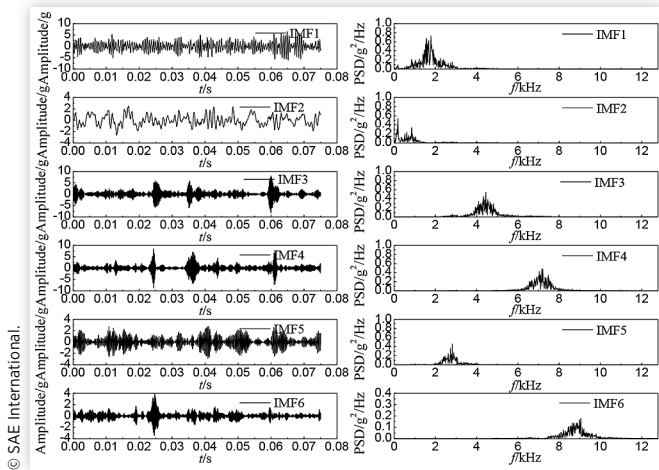
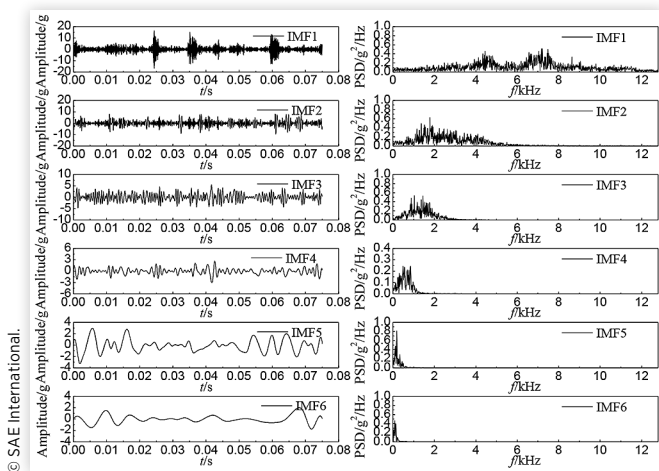


FIGURE 5 Time and frequency domain results of EMD.



IMF1 and IMF5, and there is very little information in IMF6. To simplify the result, IMF1 and IMF5 are desired to be extracted together and IMF6 can be ignored. In this section, quadratic penalty α is researched for further control of result.

The quadratic penalty α is also known as the balancing parameter of the data-fidelity constraint, which is inversely proportional to the noise in signal [13] and an inappropriate α could bring over or under decomposition to result. In original VMD, the quadratic penalty is set as a fixed value because input signal is decomposed only once. However, the adaptable VMD mentioned above adopts recursive mode to decompose different input signals several times. With the process of decomposing, noise in signal is reducing gradually, and the quadratic penalty value should increase gradually.

A novel method is proposed to select quadratic penalty values automatically: an initial quadratic penalty value is set as α_0 and the quadratic penalty value in follow-up decomposing is set as $\alpha_k = k\alpha_0$, where k is the order of decomposition level. To get an ideal result, the signal shown in Fig. 3 was decomposed under 151 different α_0 values, in which it increased from 500 to 2000 by 10. As a parameter for

describing the degree of non-Gaussian, the fourth-order cumulant of reconstructed decomposing result was taken to evaluate result. The relationship between α_0 and fourth-order cumulant is shown in Fig. 6.

As shown in Fig. 6, there are several step changes in the fourth-order cumulant. The reason is that with α_0 changing, the number of components changes. Even so, the minimum value at $\alpha_0 = 1180$ shows that irrelevant impact component and noise in signal have been filtered in the maximum extent. Although the fourth-order cumulant is falling at $\alpha_0 = 2000$, the condition of $\alpha_0 > 2000$ is not analyzed for the consideration of great difference between IMFs.

Based on that, $\alpha_k = 1180k$ was taken as the appropriate value to decompose the signal shown in Fig. 3 and the result is shown as Fig. 7.

As shown in Fig. 7, in the condition that IMFs maintain narrow bandwidth feature, the optimized VMD can extract

FIGURE 6 Relationship between α_0 and the fourth-order cumulant.

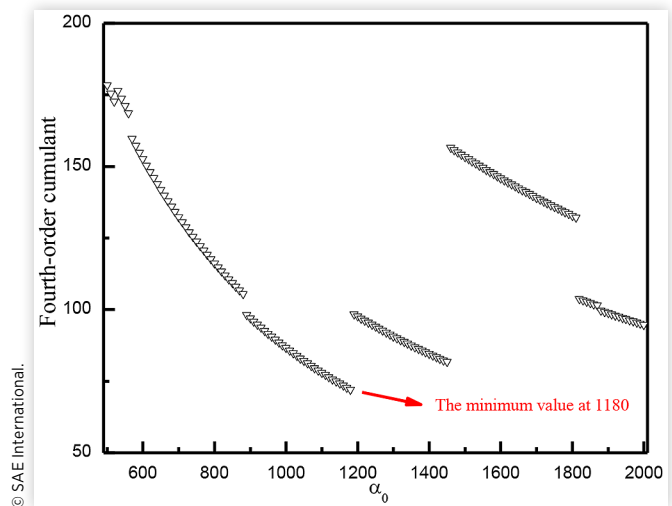
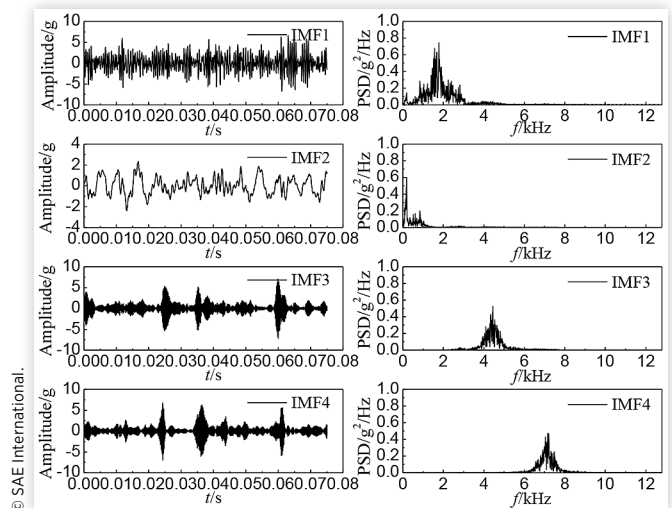


FIGURE 7 Time and frequency domain decomposition results of adaptable VMD with dynamic quadratic penalty.



similar frequency components together and filter out the component with little information. This result demonstrates that the dynamic α has advantages in extracting desired simple components.

Faults Detection Using the ESN Based on Dimension Reduction

The simple result decomposed by optimized VMD is restructured in this section to extract feature. Because of complex structure and vibration sources of engine, a single characteristic parameter cannot describe various faults clearly. For this reason, 8 characteristic parameters are selected and they are standard deviation, kurtosis, peak to peak, averaged amplitude, root mean square (RMS), Shannon entropy, the maximum singular value and the fourth-order cumulant, respectively [21].

Analysis of ESN

As an efficient ANN, ESN shows great potential in the field of machine identification. To analyze it, 4 different working conditions, including normal working condition, injection failure, small valve clearance and big valve clearance at 1600 r/min with 100% load were selected. Vibration signal near the 1st cylinder was collected to test the recognition rate of failures in the 3rd cylinder. 100 sets of signals in each working condition were decomposed, restructured and extracted feature in order to obtain 400 sets of 8-dimensional data. 50 of 100 sets in each working condition were used as training samples and the rest were used to test trained ESN.

The original result in ESN is shown as probability that samples belong to particular class, in which the maximum is taken as final recognition. For clear analysis, the original probability of testing data is shown in Fig. 8. In this paper, the reservoir size was set as 4. The 1st-50th sets of samples are corresponding to the normal working condition, the 51st-100th sets of samples are corresponding to the injection failure, the 101st-150th sets of samples are corresponding to the small valve clearance and the 151st-200th sets of samples are corresponding to the big valve clearance.

As shown in Fig. 8, the black curve is obviously higher than the others in the 1st-50th sets of samples, which shows the normal working condition can be recognized. The red curve in the 51st-100th sets of samples and the blue curve in the 101st-150th sets of samples are mostly higher than other curves respectively, which shows most injection failure and small valve clearance samples can be recognized. While the green curve does not stand out in the 151st-200th sets of samples, which means the big valve clearance samples cannot be recognized. Based on Fig. 8, final recognition results are calculated and listed in Table 3.

As shown in Table 3, the recognition result agrees with the probability curves and the overall recognition rate is 83.0%. The recognition rate is not ideal in the case of small

FIGURE 8 Result of testing data, where the black curve refers to the probability that samples belong to the normal working condition, and the red, blue and green curves correspond to the injection failure, small valve clearance and big valve clearance, respectively.

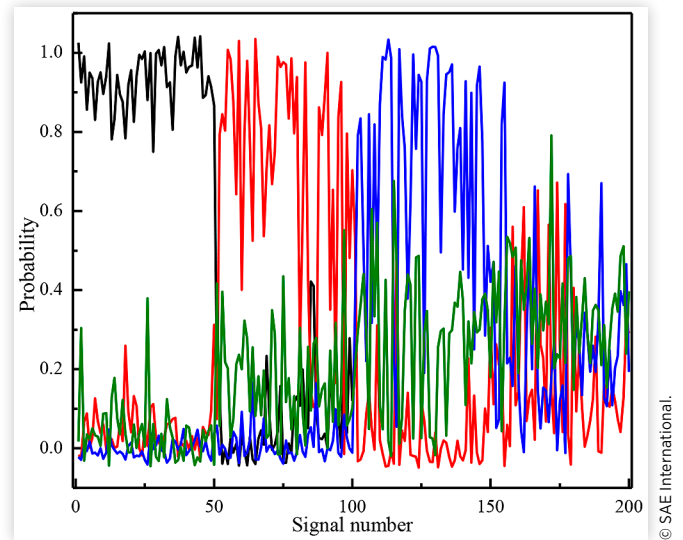


TABLE 3 Recognition result of ESN.

Working condition	Number of correct recognition
Normal working condition	50
Injection failure	43
Small valve clearance	40
Big valve clearance	33
Recognition rate	83.0%

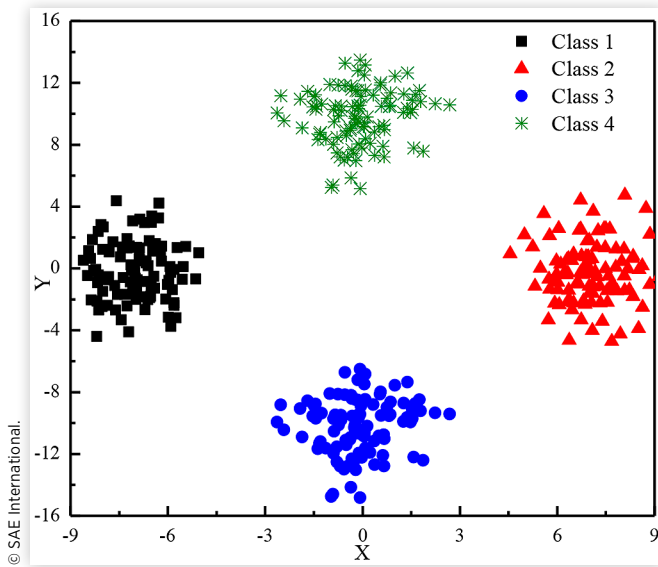
amount data, which indicates that further optimization needs doing for improving it.

Analysis of Dimension Reduction Methods

A single characteristic parameter may not describe faults clearly, while too many ones can increase the computational burden of classifier, which is one of the main reasons for the low recognition rate in last section. A dimension reduction method is introduced to improve the generalization and computational efficiency of ESN.

For clear observation and explanation, 400 sets of 2-dimensional simulated samples are used to analyze dimension reduction methods. As shown in Fig. 9, there are 100 sets of samples in each class and the samples are composed of random numbers in certain areas. Specifically, the areas of simulated samples located are scattered to make sure every characteristic parameter contributes to the description of class, which is similar to the measured signals.

The purpose of dimension reduction is to obtain low-dimensional characteristic parameter as well as retain most inner information of original data. Local Fisher discriminant analysis (LFDA) is a common used supervised linear

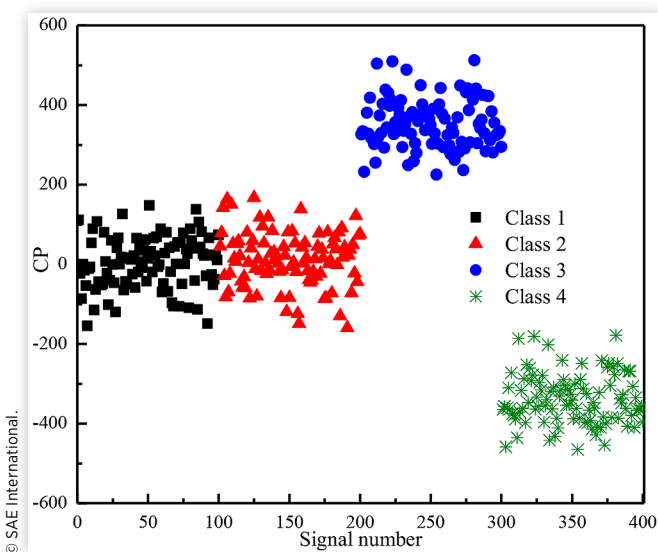
FIGURE 9 Simulated samples.

dimension reduction method [22] and the result of it is shown in Fig. 10. The 1-dimensional characteristic parameter is abbreviated as CP for no physical meaning.

As shown in Fig. 10, the samples are projected on to a plane approximating to Y axis direction, which results in the 1st and 2nd classes overlapping with each other. For the nonlinear decision boundaries of simulated samples, a LFDA method optimized by kernel function, i.e. KLFDA, is introduced to solve this problem [22]. Gaussian kernel was selected as the function and its definition is:

$$\text{Gaussian kernel} = \exp\left(-\frac{\|X - X'\|^2}{2\sigma^2}\right) \quad (11)$$

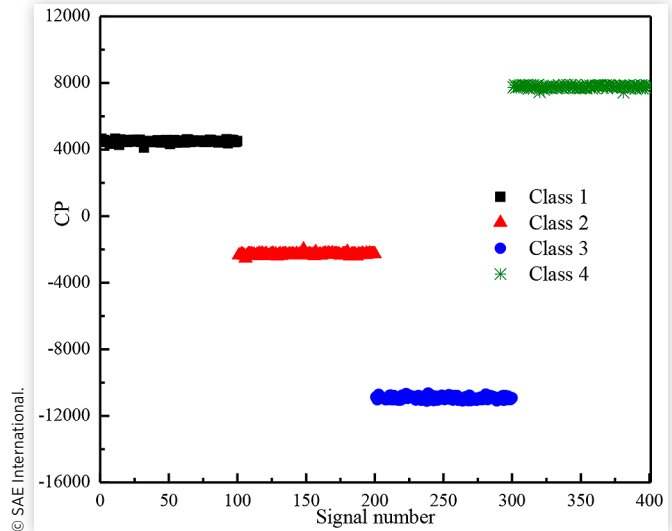
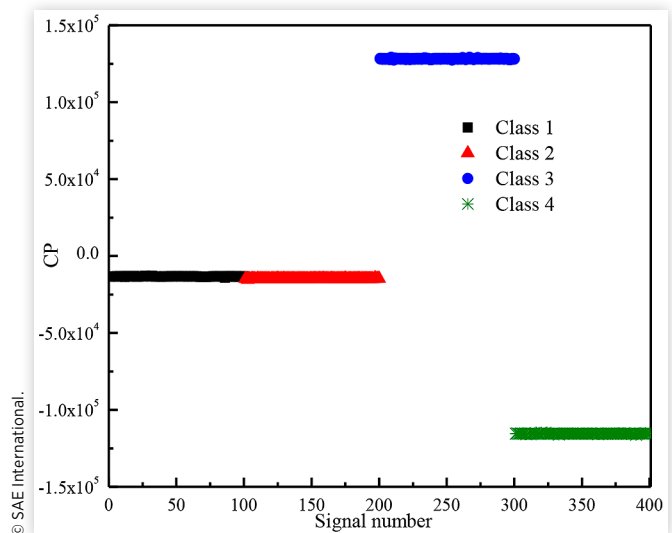
where the X refers to input data, σ is control parameter and it was selected as 2 in this paper.

FIGURE 10 Dimension reduction result of LFDA.

The dimension reduction result of KLFDA is shown as Fig. 11. Compared with the LFDA, the KLFDA with Gaussian kernel has ability to reduce the dimension of nonlinear samples appropriately. Considering the strong nonlinearity of measured signals, the KLFDA is more suited for reducing the 8-dimensional data computed from engine vibration signals.

Besides, several other kernel functions, such as sigmoid kernel, log kernel and so on, were also researched. These kernel functions cannot obtain satisfactory results, in which a representative result of log kernel is shown in Fig. 12.

As shown in Fig. 12, the KLFDA with log kernel obtains a similar result with LFDA. So the Gaussian kernel is a superior choice for this research.

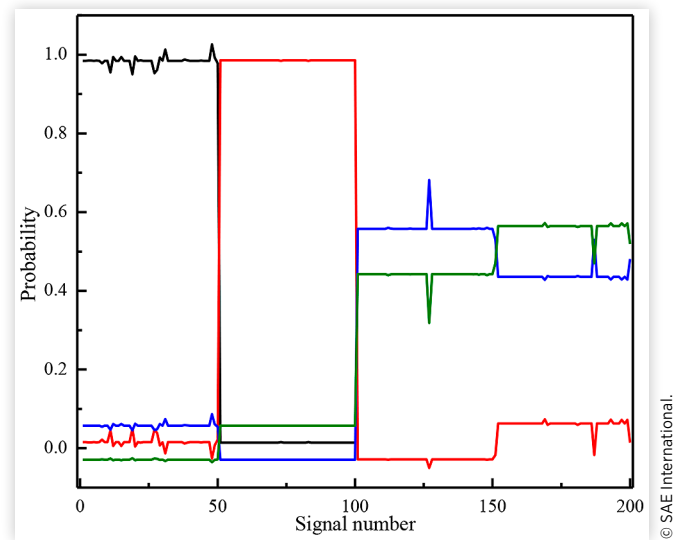
FIGURE 11 Dimension reduction result of KLFDA with Gaussian kernel.**FIGURE 12** Dimension reduction result of KLFDA with log kernel.

Faults Detection Using the ESN Based on KLFDA

Based on above analyzed, a faults detection approach using the ESN based on KLFDA is proposed. High-dimensional data is processed by KLFDA firstly and then low-dimensional data is recognized by ESN. To verify its advantages, the same measured data was processed by this approach. The probability curves of ENS are shown in Fig 13.

As shown in Fig. 13, the black and red curves are higher than others in the 1st-50th and 51st-100th sets of samples respectively and even close to 1, which shows the normal

FIGURE 13 Result of the ESN based on KLFDA, where the black curve refers to the probability that samples belong to the normal working condition, and the red, blue and green curves correspond to the injection failure, small valve clearance and big valve clearance, respectively.



working condition and the injection failure can be recognized successfully. Although the blue and green curves are lower, they are the highest in certain area, which means the small and big valve clearance can also be recognized. The recognition rate is calculated and listed in Table 4.

As shown in Table 4, only 2 sets of samples under big valve clearance are not recognized correctly and the recognition rate increases to 99.0%. This result illustrates this novel approach is superior.

To verify the necessity of extraction for 8 characteristic parameters, every single characteristic parameter was recognized by ESN. To verify the advantages of KLFDA with Gaussian kernel, the samples processed by LFDA and KLFDA with log kernel were recognized by ESN. To verify the advantages of ESN, the samples were recognized by SVM and BPNN. The recognition results are given in Table 5.

As shown in Table 5, every single characteristic parameter cannot recognize multiple engine faults accurately, which verifies the necessity to extract several characteristic parameters. The recognition rates of ESN based on LFDA and KLFDA with log kernel are 51.5% and 65%, respectively. The recognition rates of SVM and BPNN are 80.0% and 80.5%, respectively. They are all lower than 99.0% shown in Table 4. The results show the proposed novel approach can get high recognition rate and is able to detect multiple engine faults.

TABLE 4 Recognition result of ESN based on KLFDA with Gaussian kernel.

Working condition	Number of correct recognition
Normal working condition	50
Injection failure	50
Small valve clearance	50
Big valve clearance	48
Recognition rate	99.0%

TABLE 5 Comparison of different situations.

Situations		Normal working condition	Injection failure	Small valve clearance	Big valve clearance	Recognition rate
Single parameter	Standard deviation	50	40	38	18	73.0%
	Kurtosis	0	38	35	28	50.5%
	Peak to peak	28	22	36	26	56.0%
	Averaged amplitude	50	40	36	5	65.5%
	RMS	50	40	38	17	72.5%
	Shannon entropy	47	25	2	32	53.0%
	The maximum singular value	50	0	49	0	49.5%
	The fourth-order cumulant	50	2	47	0	49.5%
ESN based on LFDA		45	6	47	5	51.5%
ESN based on KLFDA with log kernel		44	33	39	14	65.0%
SVM		48	39	32	41	80.0%
BPNN		50	41	36	34	80.5%

Conclusion and Discussion

Conclusion

This paper researched a novel approach to detect multiple engine faults based on vibration signals. The main conclusions are:

1. Recursive mode is introduced to overcome the problem that the decomposing level in VMD should be selected manually and an adaptive VMD method is obtained. A dynamic quadratic penalty is proposed in adaptive VMD for that a fixed value may not extract desired components exactly. The dynamic quadratic penalty is selected as $\alpha_K = 1800k$ by data analysis method and shows ideal results.
2. Vibration signals are decomposed by optimized VMD firstly and 8 characteristic parameters of reconstructed signal are taken as input since few characteristic parameters cannot describe multiple faults clearly. While a large number of characteristic parameters bring computational burden to classifier, which results in low accuracy and efficiency. KLFDA with Gaussian kernel is used to processed high-dimensional samples in order to get 1-dimensional ones with simple structure and rich information.
3. As a promising ANN, ESN is taken as the classifier to recognize engine faults. For the struggle of ESN in high-dimensional samples recognition, the LKFDA reduces the dimension to 1, which improves the recognition rate of ESN obviously. The comparisons with others verify this method is superior.

The novel approach proposed in this paper is able to recognize multiple engine faults accurately and efficiently, and has certain theory and engineering practice significances.

Discussion and Outlook

There is much research should be done in the future:

1. In the research of KLFDA, only several kernel functions were analyzed. More kernel functions and their control parameters will be researched further in follow-up work.
2. The parameters of reservoir and activation functions have a great influence on ESN. That will be research in the future to get the best performance.

References

1. Caliskan, H., Tat, M.E., and Hepbasil, A., "A Review on Exergetic Analysis and Assessment of Various Types of Engines," *International Journal of Exergy* 7(3):287-311, 2010, doi:10.1504/IJEX.2010.031986.
2. Nahim, H.M., Younes, R., Shraim, H., and Ouladsine, M., "Oriented Review to Potential Simulator for Faults Modeling in Diesel Engine," *Journal of Marine Science and Technology* 21(3):533-551, 2016, doi:10.1007/s00773-015-0358-6.
3. Li, Z.X., Jiang, Y., Duan, Z.H., and Peng, Z.X., "A New Swarm Intelligence Optimized Multiclass Multi-Kernel Relevant Vector Machine: An Experimental Analysis in Failure Diagnostics of Diesel Engines," *Structural Health Monitoring: An International Journal* 17(6):1503-1519, 2018, doi:10.1177/1475921717746735.
4. Zhang, M.Q., Zi, Y.Y., Niu, L.K., Xi, S.T., and Li, Y.Q., "Intelligent Diagnosis of V-Type Marine Diesel Engines Based on Multifeatures Extracted from Instantaneous Crankshaft Speed," *IEEE Transactions on Instrumentation and Measurement* 99:1-19, 2018, doi:10.1109/TIM.2018.2857018.
5. Wakiru, J.M., Pintelon, L., Muchiri, P., and Chemweno, P., "A Review on Lubricant Condition Monitoring Information Analysis for Maintenance Decision Support," *Mechanical Systems and Signal Processing* 118:108-132, 2018, doi:10.1016/j.ymsp.2018.08.039.
6. Giancarlo, C., Ornella, C., Fulvio, P., and Andrea, P., "Diagnostic Methodology for Internal Combustion Diesel Engines via Noise Radiation," *Energy Conversion and Management* 89:34-42, 2015, doi:10.1016/j.enconman.2014.09.055.
7. Ahmad, T.A. and Alireza, M., "Fault Detection of Injectors in Diesel Engines Using Vibration Time-Frequency Analysis," *Applied Acoustics* 143:48-58, 2019, doi:10.1016/j.apacoust.2018.09.002.
8. Sharma, A., Sugumaran, V., and Devasenapati, S.B., "Misfire Detection in an IC Engine Using Vibration Signal and Decision Tree Algorithms," *Measurement* 50:370-380, 2014, doi:10.1016/j.measurement.2014.01.018.
9. Alireza, Z.H., Saeed, A.R., Farzad, S., and Moosa, A., "Fault Detection and Diagnosis of a 12-Cylinder Trainset Diesel Engine Based on Vibration Signature Analysis and Neural Network," *Proceedings of the Institution of Mechanical Engineers, Part C: Journal of Mechanical Engineering Science* 233(6):1910-1923, 2019, doi:10.1177/0954406218778313.
10. Bi, F.R., Ma, T., and Zhang, J., "Knock Feature Extraction in Spark Ignition Engines Using EEMD-Hilbert Transform," SAE Technical Paper 2016-01-0087, 2016, doi:https://doi.org/10.4271/2016-01-0087.
11. Zheng, J.D., Cheng, J.H., and Yang, Y., "A Rolling Bearing Diagnosis Approach Based on LCD and Fuzzy Entropy," *Mechanism and MACHINE THEORY* 70:441-453, 2013, doi:10.1016/j.mechmachtheory.2013.08.014.
12. Yeh, J.R., Shieh, J.S., and Huang, N.E., "Complementary Ensemble Empirical Mode Decomposition: A Novel Noise Enhanced Data Analysis Method," *Advances in Adaptive Data Analysis* 2(2):135-156, 2010, doi:10.1142/S1793536910000422.
13. Dragomiretskiy, K. and Zosso, D., "Variational Mode Decomposition," *IEEE Tran on Signal Processing* 62(3):531-544, 2014, doi:10.1109/TSP.2013.2288675.

14. Ren, G., Jia, J.D., Mei, J.M., Jia, X.Y. et al., "An Improved Variational Mode Decomposition Method and Its Application in Diesel Engine Fault Diagnosis," *Journal of Vibroengineering* 20(6):2363-2378, 2018, doi:[10.21595/jve.2018.19694](https://doi.org/10.21595/jve.2018.19694).
15. Bi, X.Y., Cao, S.Q., and Zhang, D.M., "A Variety of Engine Faults Detection Based on Optimized Variational Mode Decomposition-Robust Independent Component Analysis and Fuzzy C-Mean Clustering," *IEEE Access* 7:27756-27768, 2019, doi:[10.1109/ACCESS.2019.2901680](https://doi.org/10.1109/ACCESS.2019.2901680).
16. Wang, B.J., Zhang, X.L., Sun, C., and Chen, X.F., "A Quantitative Intelligent Diagnosis Method for Early Weak Faults of Aviation High-Speed Bearings," *ISA Transactions* 93:370-383, 2019, doi:[10.1016/j.isatra.2019.03.011](https://doi.org/10.1016/j.isatra.2019.03.011).
17. Zheng, T.X., Zhang, Y., Li, Y.F., and Chen, L.C., "Real-Time Combustion Torque Estimation and Dynamic Misfire Fault Diagnosis in Gasoline Engine," *Mechanical Systems and Signal Processing* 126:521-535, 2019, doi:[10.1016/j.ymsp.2019.02.048](https://doi.org/10.1016/j.ymsp.2019.02.048).
18. Herbert, J. and Harald, H., "Harnessing Nonlinearity: Predicting Chaotic Systems and Saving Energy in Wireless Communication," *Science* 304(5667):78-80, 2004, doi:[10.1126/science.1091277](https://doi.org/10.1126/science.1091277).
19. Herbert, J., Mantas, L., Dan, P., and Udo, S., "Optimization and Applications of Echo State Networks with Leakyintegrator Neurons," *Neural Networks* 20:335-352, 2007, doi:[10.1016/j.neunet.2007.04.016](https://doi.org/10.1016/j.neunet.2007.04.016).
20. Bi, F.R., Li, X., Liu, C.C., Tian, C.F. et al., "Knock Detection Based on the Optimized Variational Mode Decomposition," *Measurement* 140:1-13, 2019, doi:[10.1016/j.measurement.2019.03.042](https://doi.org/10.1016/j.measurement.2019.03.042).
21. Bi, F.R., Li, X., Lin, J.W., Bi, X.B. et al., "Knock Detection Based on Recursive Variational Mode Decomposition and Multilevel Semi-Supervised Local Fisher Discriminant Analysis," *IEEE Access* 7:1-13, 2019, doi:[10.1109/ACCESS.2019.2937571](https://doi.org/10.1109/ACCESS.2019.2937571).
22. Sugiyama, M., "Dimensionality Reduction of Multimodal Labeled Data by Local Fisher Discriminant Analysis," *Journal of Machine Learning Research* 8:1027-1061, 2007, doi:[10.1007/s10846-007-9130-4](https://doi.org/10.1007/s10846-007-9130-4).

Contact Information

Fengrong Bi

State Key Laboratory of Engines, Tianjin University, Tianjin 300072, China

fr_bi@tju.edu.cn

Xin Li

State Key Laboratory of Engines, Tianjin University, Tianjin 300072, China

nvh_lixin@tju.edu.cn

Acknowledgments

The authors gratefully acknowledge the Project 18JCYBJC20000 supported by the Natural Science Foundation of Tianjin.

Definitions/Abbreviations

EMD - Empirical Mode Decomposition

VMD - Variational Mode Decomposition

PSD - Power Spectral Density

IMF - Intrinsic Mode Function

ESN - Echo State Network

LFDA - Local Fisher Discriminant Analysis

KLFDA - Kernel Local Fisher Discriminant Analysis

RMS - Root Mean Square

SVM - Support Vector Machine

BPNN - Back Propagation Neural Network